Flow and mixing dynamics in a patterned wetland: Kilometer-scale tracer releases in the Everglades

Evan A. Variano,[1,2] David T. Ho,[1,3] Victor C. Engel,[4] Paul J. Schmieder,[1] and Matthew C. Reid[1,5]

[1] Surface water flow dynamics in the Florida Everglades were investigated using sulfur hexafluoride tracer releases, from which advection and dispersion were determined. Several sites were studied, each characterized by different vegetation patterns and proximity to hydrologic control structures. The measured flow directions suggest that basin-scale forcing from water management structures and operations can override the effects of local landscape features in guiding the flow. Management effects were particularly evident in two regions where the historic, natural landscape patterning has degraded. The large spatial scale over which tracer data were collected allows the dispersion rate to be determined at unprecedented spatial scales. These measurements showed much larger dispersion coefficients than reported by previous experiments at smaller scales. This finding and a measurement of the drag due to vegetation over large scales are of interest to Everglades water resource managers concerned with the transport of sediment and biologically active solutes such as phosphorous.

Citation: Variano, E. A., D. T. Ho, V. C. Engel, P. J. Schmieder, and M. C. Reid (2009), Flow and mixing dynamics in a patterned wetland: Kilometer-scale tracer releases in the Everglades, *Water Resour. Res.*, *45*, W08422, doi:10.1029/2008WR007216.

1. Introduction

[2] Advection and dispersion play an important role in wetland ecology by influencing nutrient fluxes, soil processes, and vegetation dynamics. The past century of agriculture and urban development surrounding the Florida Everglades has subjected this 1.5 million hectare wetland to periodic drainage, impoundment, and/or excessive nutrient releases [*Grunwald*, 2006]. These changes in hydrodynamics and nutrient budgets have been accompanied by changes in vegetative communities and wildlife habitats. Understanding the causal links between these changes is of interest for current efforts to restore or maintain some aspects of the historical Everglades ecosystem.

[3] A defining characteristic of the historic Everglades was the wide expanse of shallow slow-moving oligotrophic surface water termed sheet flow. In the areas where sheet flow occurred, the vegetation often formed a characteristic ridge and slough patterning, where sawgrass (*Cladium jamaicense*) ridges are separated by deeper water sloughs that support submerged (e.g., *Utricularia* spp.), floating (*Nymphaea* spp.) and emergent (*Eleocharis* spp. and *Panicum* spp.) vegetation.

The peat formations underlying the sawgrass ridges are slightly elevated compared to the sloughs.

[4] Ridges and sloughs in the Everglades are aligned parallel to the historic flow direction [*National Research Council*, 2003], and therefore sheet flow is thought to have played a role in their formation [*Larsen et al.*, 2007]. This hypothesis is supported by observations of degraded ridge and slough patterning in regions where the volume, timing, or velocity of sheet flow have been disrupted. In over-drained areas, sawgrass has expanded into the sloughs, and in impounded areas, slough vegetation replaces sawgrass with a loss of patterning. The peat surface elevation differences between the sawgrass ridges and sloughs also vary with the hydrologic setting and history of disturbance [*Givnish et al.*, 2008].

[5] Flow dynamics and vegetation populations are closely linked in the Everglades. Vegetation creates a spatially variable source of drag, thus advection and dispersion are likely to differ between well preserved and degraded regions. Altered flow velocities, particularly in the impounded zones, are likely to affect the suspension and transport of sediment and organic matter that maintain ridge structure [*Larsen et al.*, 2007]. Dispersion rates are likely sensitive to changes in vegetation densities associated with altered water depths, and can influence the rate at which excess nutrients are distributed through the system [*Noe and Childers*, 2007].

[6] Dispersion associated with pipe, open channel, and groundwater flows can be quantified using stochastic models [*Taylor*, 1954; *Fischer et al.*, 1979; *Gelhar*, 1993]. In wetlands, such modeling efforts are complicated by the lack of data on the diffusion rates and spatial variation of velocity fields that cause dispersion. *Nepf et al.* [1997a] collected such data using laboratory measurements in model wetlands, from which they derived a wetland dispersion model. This model

[1]Lamont-Doherty Earth Observatory, Earth Institute at Columbia University, Palisades, New York, USA.
[2]Now at Department of Civil and Environmental Engineering, University of California, Berkeley, California, USA.
[3]Now at Department of Oceanography, University of Hawaiʻi at Mānoa, Honolulu, Hawaii, USA.
[4]South Florida Natural Resources Center, Everglades National Park, Homestead, Florida, USA.
[5]Now at Department of Civil and Environmental Engineering, Princeton University, Princeton, New Jersey, USA.
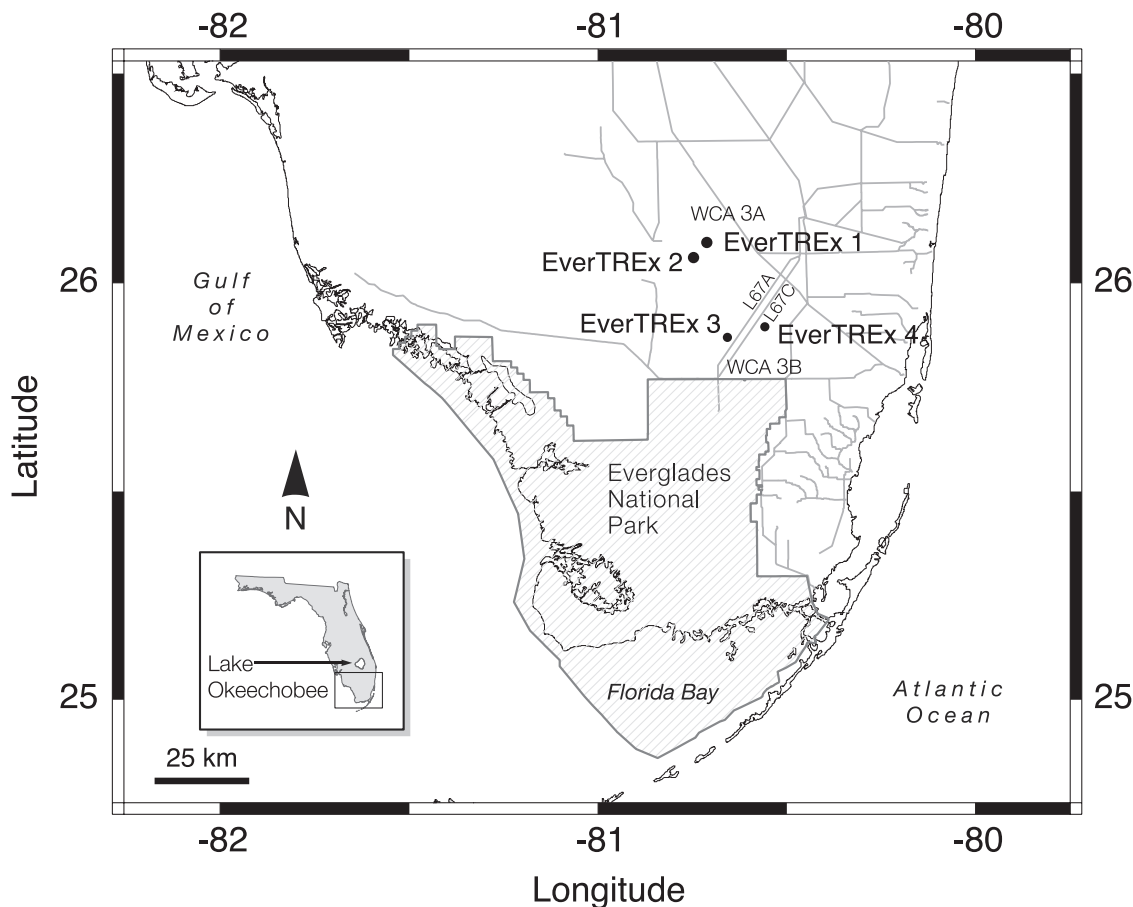
Figure 1. Schematic view of the ridge and slough region of the Everglades, including the L67 levee-canal system and the sites of EverTREx 1–4. The hashed area denotes Everglades National Park.

applies to flows with higher Reynolds number than those typically found in the Everglades. Detailed velocity measurements in the Everglades by *Harvey et al.* [2009] promise to yield similar advances in the creation of dispersion models applicable to slow-flowing and patterned wetlands. In the absence of such models, dispersion in the Everglades has been measured directly with tracer releases [*Saiers et al.*, 2003; *Harvey et al.*, 2005; *Dierberg et al.*, 2005].

[7] Tracer releases in wetlands and other systems have shown that the dispersion coefficient can increase with time, even under steady and homogeneous conditions [*Fischer et al.*, 1979; *Sabol and Nordin*, 1978; *Young and Jones*, 1991]. Such "anomalous dispersion" occurs when the history of velocities experienced by any given tracer particle is not an accurate representation of the spatiotemporal velocity distribution of the flow. This can happen if too little time has passed for the Fickian limit to be reached. Alternately, anomalous dispersion occurs when a growing plume encompasses regions of successively greater velocity variance. When present, such a process makes it difficult to predict dispersion rates at large scales from measurements made at small scales. The large-scale measurements presented here are intended to aid in the creation of dispersion models for patterned wetlands that build on the diffusion models of Fick, Taylor and others [*Fischer et al.*, 1979].

[8] The Everglades Tracer Release Experiment (EverTREx), introduced by *Ho et al.* [2009] and discussed here, is designed to measure advection and dispersion at large spatial

scales in both degraded and relatively well-preserved areas. This was accomplished with a series of sulfur hexafluoride (SF_6) tracer releases at scales that included multiple sawgrass ridges and sloughs. The advection and dispersion values derived from these data include the aggregate effect of landscape patterning, and provide a complement to previous studies at smaller scales [*Saiers et al.*, 2003; *Lee et al.*, 2004; *Harvey et al.*, 2005; *Bazante et al.*, 2006; *Solo-Gabriele*, 2008; *Huang et al.*, 2008]. To date, four EverTREx campaigns have been held. EverTREx 1 and 2 have been examined by *Ho et al.* [2009], including some basic calculations of advection and dispersion. The present contribution includes EverTREx 3 and 4, and builds on the work of *Ho et al.* [2009] by considering variations in hydrodynamics between well-preserved and degraded portions of the landscape, and by examining in greater detail the dispersion processes in the patterned landscape.

2. Study Locations

[9] The studies discussed herein occurred near the geographic center of the Everglades, halfway between its source waters at Lake Okeechobee and its eventual outflow to Florida Bay (Figure 1). In this region, the landscape is divided by a system of levees and canals, with flows managed by gates and pumps. EverTREx 1 was a pilot experiment that allowed for testing and refinement of experimental methods [*Ho et al.*, 2009]. EverTREx 2–4 focused on three regions
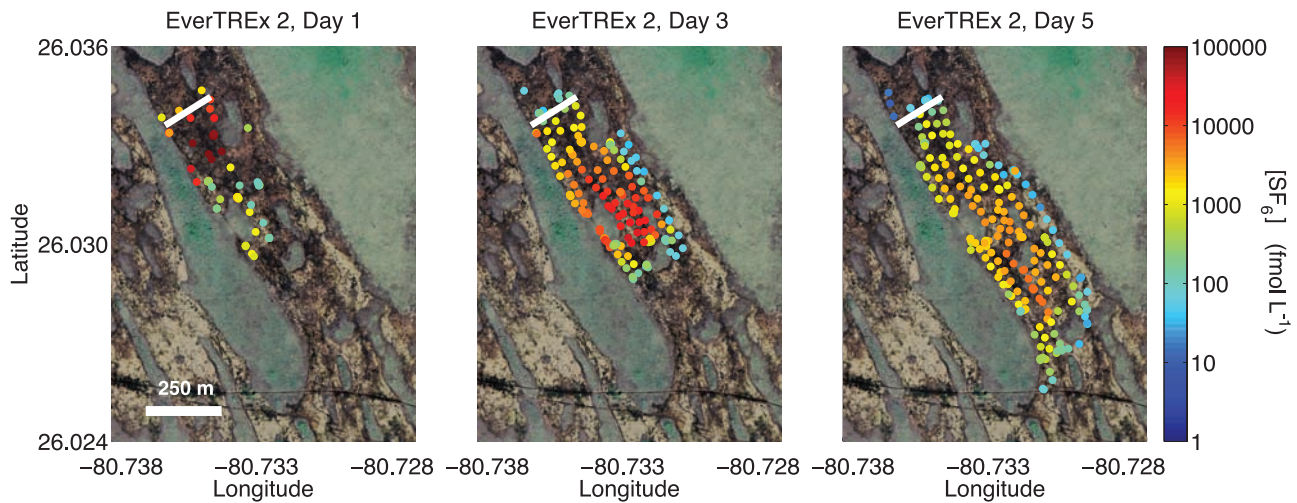
Figure 2. Selected tracer measurements from EverTREx 2. Green areas are ridges, and black or tan areas are sloughs. Each colored point represents a single tracer measurement. Blue dots are near zero concentration and thus represent bounds to the plume's extent. Complete tracer measurements for EverTREx 2 are available in work by *Ho et al.* [2009].

which have been affected by the levee-canal system L67 to varying degrees. The L67 system consists of two parallel canal-levee pairs which route flow to the southwest, and divide Water Conservation Area 3 (WCA 3) into WCA 3A and 3B (Figure 1). The northern canal, L67A, is connected to other canals and is controlled at both ends by pumps and gates. The southern canal, L67C, is not connected to any other canals or controls and thus has a more passive effect on flows. A gap exists in L67C, presenting an area of reduced resistance to flow. This gap is useful to study as a prototype for other levee breaches proposed as part of Everglades restoration efforts.

[10] EverTREx 2–4 were performed during wet season conditions, summarized in Tables 1 and 2. EverTREx 2 was performed in WCA 3A, in a region where the landscape has maintained the traditional patterning [*Ho et al.*, 2009]. Here, ridges and sloughs are $\mathcal{O}(1)$ km in length, and 50–500 m in width (Figure 2).

[11] EverTREx 3 was performed in WCA 3A just northwest of L67A, where water depths are elevated because of impoundment by the L67 system. The landscape there has distinct ridges and sloughs, but these are much smaller than those in traditional ridge and slough landscapes, and have a winding, sinuous shape (Figure 3).

[12] EverTREx 4 was performed in WCA 3B, southeast of the gap in L67C. Because of artificially low water levels and short hydroperiods in this region, ridge vegetation has gradually invaded the sloughs in WCA 3B. The remaining sloughs are small and typically aligned with the historical flow direction (south-southeast) (Figure 4).

[13] In addition to vegetation differences, ridges and sloughs have different peat thickness that results in different water depths and hydrodynamics in the two community types (Table 3). Water depths were measured at each EverTREx site using a surveying staff to take three replicate depth measurements within a 1 m^2 quadrat. Average depths were calculated using 20 randomly located quadrats in the ridges and sloughs. The differences in peat surface elevations were calculated from the set of depth measurements in each of the two habitats. The site of EverTREx 2 displayed a significant difference between ridge and slough elevation, and in this way resembles the historic, or undisturbed, patterned landscape (Science Coordination Team, The role of flow in the Everglades ridge and slough landscape, 2003, South Florida Ecosystem Restoration Task Force, Miami, Florida, available at http://sofia.usgs.gov/publications/papers/sct_flows). The site of EverTREx 3 also displayed significant differences, albeit with greater variance. The site of EverTREx 4 lacked clear elevation differences between ridges and sloughs (Table 3).

3. Methods

3.1. Tracer Measurements

[14] The SF$_6$ tracer methods were applied as described by *Ho et al.* [2002, 2009]. For each experiment, SF$_6$ gas was used to saturate 8 L of water, which was then injected at the study site as a near-instantaneous line release that covered the entire depth of the water column. During the experiments, the tracer concentration field evolved because of advection, dispersion, and air-water gas exchange.

Table 1. Locations of EverTREx Campaigns

Field Campaign	Latitude (deg N)	Longitude (deg W)	Dates
EverTREx 1	26.075180	80.711496	23 Jul to 1 Aug 2006
EverTREx 2	26.034098	80.735926	29 Nov to 5 Dec 2006
EverTREx 3	25.851181	80.649714	10–21 Oct 2007
EverTREx 4	26.029698	80.733141	24–30 Oct 2007

Table 2. Physical Characteristics of the Study Sites

Field Campaign	Mean Depth (cm)	Landscape Pattern
EverTREx 1	31	parallel ridge and slough
EverTREx 2	42	parallel ridge and slough
EverTREx 3	75	nondirectional and fractalline
EverTREx 4	46	small remnant sloughs only
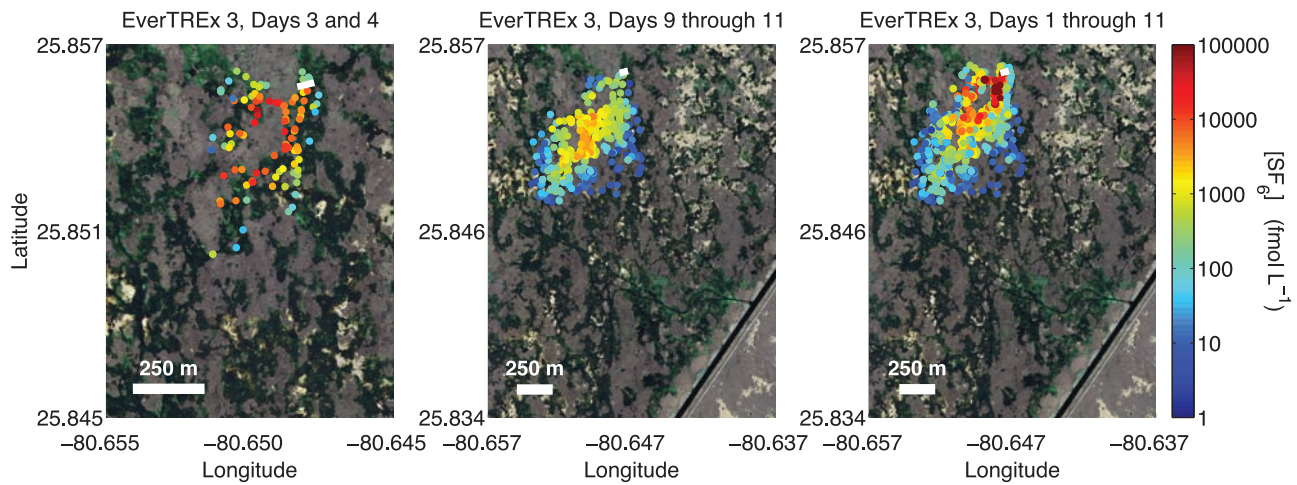
Figure 3. Selected tracer measurements from EverTREx 3. Grey areas are ridges, and green areas are sloughs. Each colored point represents a single tracer measurement. Blue dots are near zero concentration and thus represent bounds to the plume's extent. Note that the left plot shows a smaller spatial region than the others and the right plot shows a composite over the entire measurement period, similar to a streak line. The L67A canal and levee are visible in the southeast corner.

[15] The real-time continuous SF_6 analysis system described by *Ho et al.* [2002, 2009] was mounted on an airboat and used to measure the concentration of SF_6 dissolved in the water column. The detection limit was 10 fmol L^{-1}, thus the system could detect SF_6 concentrations that had been diluted by a factor of $\mathcal{O}(10^6)$ relative to the initial concentration injected at the tracer release line. Uncertainties are discussed by *Ho et al.* [2009], and for the experiments presented here were ±2% in concentration and ±5 m in position. Sampling locations were selected on the basis of the accumulated observations of the evolving tracer distribution.

3.2. Vertical Structure

[16] The analyses presented here approximate the flow as vertically homogeneous. In marsh flows, the vertical velocity profile is dominated by variations in vegetation density [*Bazante et al.*, 2006; *Leonard and Croft*, 2006; *Lightbody and Nepf*, 2006]. This vegetation effect overwhelms that of the bed and surface boundary layers, which are quite small (on the order of one vegetation diameter) even for sparse vegetation [*Nepf et al.*, 1997a].

[17] The assumption of vertical homogeneity was tested with an acoustic Doppler current profiler (HR Profiler, NortekUSA). Measurements were made during November 2007 near the tracer release location of EverTREx 4 (25.901121°N, 80.565263°W), and also in a slough near the center of WCA 3B (25.876278°N, 80.534523°W) which was 4.25 km from the release location in the direction of measured flow. Average velocities (U being streamwise, V cross stream, and W vertical) were computed over 30-min
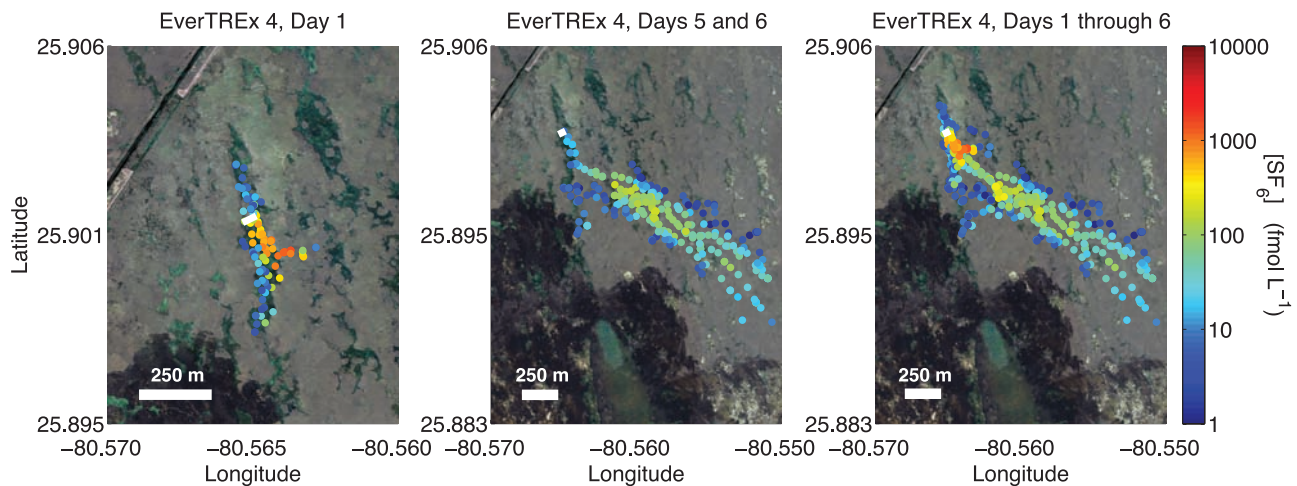
Figure 4. Selected tracer measurements from EverTREx 4. Grey areas are ridges, and green areas are sloughs, other than the recently burned region visible in the southwest corner of each image, which appears black and surrounds a green tree island. Each colored point represents a single tracer measurement. Blue dots are near zero concentration and thus represent bounds to the plume's extent. Note that the left plot shows a smaller spatial region than the others and the right plot shows a composite over the entire measurement period, similar to a streak line. The L67C canal and levee, including the gap in the levee, are visible in the northwest corner.

Table 3. Peat Elevation Differences at the Study Sites

Field Campaign	Ridge-Slough Elevation Difference (cm)
EverTREx 2	16 ± 4
EverTREx 3	15 ± 13
EverTREx 4	6 ± 6

Table 4. Angles of Measured Flow Direction and Local Landscape Pattern[a]

Field Campaign	Tracer Heading (deg)	Landscape Orientation (deg)
EverTREx 2	147 ± 6	150
EverTREx 3	214 ± 1	169
EverTREx 4	131 ± 2	167

[a]Angles are north $\equiv 0°$, east $\equiv 90°$. The value for EverTREx 3 is based on a nearby tree island that has not lost its historical structure.

intervals. The velocity profiles seen in Figure 5 suggest vertical homogeneity in the subsection of the water column that was measured.

[18] To ensure that the tracer data collected during EverTREx were vertical averages, water samples were drawn from an intake creating a diffuse, omnidirectional potential flow at middepth. In addition, vertical mixing by thermal convection (solar heating of the peat occurs in the typical Everglades water column which is shallow and clear) and wind shear (in locations where the water surface is not sheltered by emergent vegetation) can lead to a vertically homogeneous tracer distribution.

4. Results

4.1. Flow Direction

[19] Figures 2, 3, and 4 show SF_6 concentrations at each location sampled. The main axis of the tracer plume (found via a 2-D Gaussian fit, Table 4) indicates surface water flow direction [*Ho et al.*, 2009]. In the well-preserved landscape studied in EverTREx 2, the overland flow measured via tracer release was aligned with the hydraulic gradient and the longitudinal axes of the local ridges and sloughs. In contrast, in the degraded landscape studied in EverTREx 3 and 4, the flow was not aligned with the local landscape patterning.
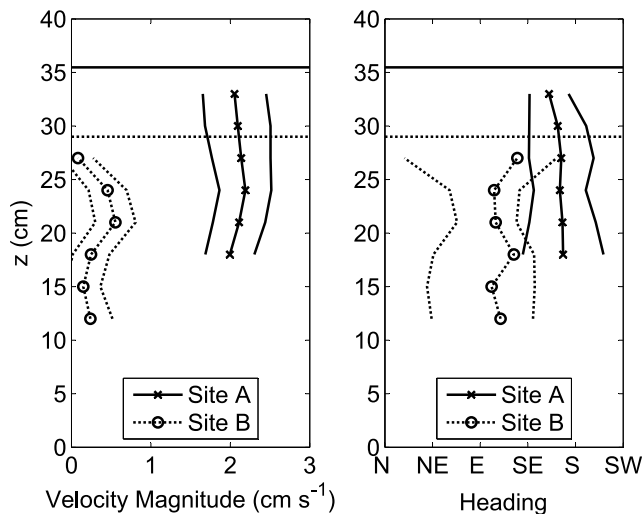
Figure 5. Vertical profile of the time-averaged horizontal velocity magnitude $\sqrt{U^2 + V^2}$ at two sites. Site A was near the tracer release location for EverTREx 4, and site B was 4.25 km downstream. Vertical velocities (not shown) were statistically identical to zero. Height $z \equiv 0$ at the bed, and horizontal lines show the location of the water surface for the two cases. Bounding lines are the 95% confidence intervals. These data were captured by an upward looking HR Profiler resting on the peat surface; thus, the lower portion of the water column was not measured.

Instead, it was aligned with the hydraulic gradients set up by the water levels at the boundaries of WCA3 and by the influence of nearby control structures such as L67. For example, during EverTREx 3 the flow direction was aligned with L67A, whose heading is 215°. While flowing in this southwesterly direction, the tracer crossed both large and small ridges. Similarly, in EverTREx 4 the tracer traveled through large expanses of sawgrass, and appeared to be unaffected by the presence of isolated sloughs. The flow direction during EverTREx 4 was aligned with the direction of surface water flowing through the gap in the nearby L67C levee, and with the hydraulic gradient set by the border canals.

4.2. Advection and Dispersion

[20] Advection and dispersion rates were determined from the data using a combination of models that were selected on the basis of observations of the tracer distributions. For example, EverTREx 2 showed the long tail indicative of anomalous diffusion (quantified by a statistically significant negative skewness computed from a transect along the main axis of the plume). Therefore, the model for EverTREx 2 includes processes that represent non-Fickian dispersion, while the model for EverTREx 3 and 4 uses the standard Fickian dispersion term.

[21] All models discussed here assume that the flow properties (including drag and dispersion rate) are spatially homogeneous. This is justified a priori by noting that the plumes either cross many ridges (EverTREx 3) or stay primarily within a single vegetation regime (EverTREx 2 and 4), thus the landscape is essentially homogeneous at the scale of the plumes. The approximation is justified a posteriori by noting that the models reproduce the tracer measurements well.

[22] The models discussed here also assume that the flow remains constant over the experimental time period. This assumption is justified by the observation of steady values for key hydrodynamic forcings, namely, water depth h and hydraulic gradient ($\partial\eta/\partial x$), where the water surface elevation η is defined with respect to the North American vertical datum (NAVD88). Gauge data from the U.S. Geological Survey Everglades Depth Estimation Network (EDEN, http://sofia.usgs.gov/eden/) shows that for EverTREx 2, 3 and 4, depth remained essentially constant over time. Specifically, the maximum daily variation of depth at each site was 0.8% and the median daily variation was 0.1%. Similarly, the hydraulic gradients remained constant. During EverTREx 2 the maximum daily variation in hydraulic gradient was 2.4% and the median daily variation was 1.3%. EverTREx 4 showed a maximum daily variation of 4.8% and a median daily variation of 0.8%. The hydraulic gradients for EverTREx 2 were computed using central differences over the 400 m grid given by the EDEN daily water surface product [*Ho et al.*, 2009]. The hydraulic gradients for EverTREx 4

were calculated from three gauges bounding the experimental site. Because EverTREx 3 was located near the L67 canal which divides the region into different hydrologic basins, the hydraulic gradient could not be measured using these methods, though the stability of depth at the site was confirmed from local gauges. This stability of external forcing during EverTREx 2–4 supports the application of steady advection and dispersion models.

4.2.1. Model of EverTREx 2 Before the Fickian Limit

[23] A transient storage model [*Deans*, 1963; *Bencala and Walters*, 1983; *Wagner and Harvey*, 1997] was used to describe the time-dependent plume growth rate and long tail observed in EverTREx 2. In this model, the flow is separated into "free" and "trapped" domains, the latter having zero velocity and the former having a mean velocity U_F. The volume ratio of the two domains is β, and they exchange mass at a rate α. This exchange has not, by definition, reached the Fickian limit, and thus leads to time-dependent spreading and non-Gaussian plume shape. The model also includes a term that describes plume spreading due to all those processes that have reached the Fickian limit, parameterized by a steady diffusion coefficient D_x. The three parameters, α, β, and D_x, replace the need for a time-dependent dispersion coefficient K_x. When all dispersion processes have reached the Fickian limit, the transient storage model simplifies to the traditional advection-dispersion equation with a steady K_x.

[24] An additional term is included in the model to account for the tracer that is lost to air-water gas exchange. This loss term is based on the standard gas exchange model, namely,

$$F = k_{SF6}\Delta C = k_{SF6}(C_{water} - \alpha_0 C_{air}), \qquad (1)$$

where F is the flux from the water to the air, k_{SF6} is the gas transfer velocity for SF_6, C_{water} is the aqueous concentration of SF_6, α_0 is the Ostwald solubility, and C_{air} is the concentration of SF_6 in air. At 25°C, $\alpha_0 = 0.006$ [*Bullister et al.*, 2002]. $C_{air} \approx 7$ parts per trillion (NOAA, http://www.esrl.noaa.gov/gmd/hats/). For each data set, $C_{water} \gg \alpha_0 C_{air}$, thus the approximation $\Delta C \approx C_{water}$ is made. For EverTREx data, this approximation results in less than 1% error in k_{SF6}.

[25] The resulting model is the Storage–Advection–Gas Exchange–Diffusion (SAGED) model. The terms on the right-hand side of equation (2) describe each of these effects in order:

$$\frac{\partial C_F}{\partial t} = \alpha(C_T - C_F) - U_F \frac{\partial C_F}{\partial x} - \frac{k_{SF6}}{h} C_F + D_x \frac{\partial^2 C_F}{\partial x^2} \qquad (2)$$

$$\frac{\partial C_T}{\partial t} = \alpha\beta^{-1}(C_F - C_T), \qquad (3)$$

where

C_F SF_6 concentration in free volume;
C_T SF_6 concentration in trapped volume;
U_F advection (speed) in free volume;
D_x rate of Fickian diffusion;
α exchange rate between free and trapped volumes;
β ratio of trapped volume to free volume;
k_{SF6} SF_6 gas transfer velocity.

This set of equations is used with Dirichlet boundary conditions and a Dirac delta function initial condition having mass M_0.

[26] The SAGED model is presented in one spatial dimension, which is appropriate for EverTREx 2 because the release line was wide and perpendicular to the flow direction. Analysis is performed on the tracer data collected within ±50 m of the slough centerline, where C is observed to be laterally homogeneous. The model gives a concentration field having many of the features typical of pre-Fickian dispersion, despite the fact that a spatially homogenous "trapped" region is not an accurate description of the factors that actually cause dispersion, namely, a spatially heterogeneous distribution of nonzero velocities correlated with vegetation structure. Since the sampling scheme was unbiased with respect to these features, and since there were no inaccessible portions of the water column where the samples were taken, the field measurements are compared to the model using volume-averaged concentrations $C = (C_F + \beta C_T)/(1 + \beta)$ and velocity $U = U_F/(1 + \beta)$.

[27] Figure 6 and Table 5 show the results of the SAGED model when it is numerically integrated and the parameters are fit to EverTREx 2 data. The reduced χ^2 value for the fit shown in Figure 6 is 0.7354. Model performance can also be evaluated by the Damkohler index (Da), which indicates whether the transient storage dynamics provide a unique and useful extension to the traditional advection-dispersion model [*Wagner and Harvey*, 1997]. The Damkohler index is a ratio of advection time scales to storage residence time scales: $Da \equiv \alpha \left(1 + \beta^{-1}\right) \mathcal{L}/U_F$, where $\mathcal{L}$ is the distance of downstream transport, taken here to be 750 m. The model used for EverTREx 2 gives $Da = 4.8$, which indicates that the parameter set is unique, being of $\mathcal{O}(1)$ [*Harvey and Wagner*, 2000]. Following *Wagner and Harvey* [1997] the value of Da can also be used to deduce approximate uncertainties in the transient storage parameters, which for EverTREx 2 are ≈30% in α and ≈20% in β.

[28] These results are complementary to the analysis performed by *Ho et al.* [2009]. There, a Gaussian plume model was fit to data for each day in EverTREx 2. The Gaussian peak showed a mean velocity over days 1–3 of 0.147 ± 0.001 cm s^{-1} and a mean velocity over days 4–6 of 0.075 ± 0.004 cm s^{-1}. The time-dependent K_x (which includes both the effect of D_x and transient storage) is measured by *Ho et al.* [2009] to be bounded by 370 ± 140 cm^2 s^{-1} (average over days 1–3) and 2600 ± 300 cm^2 s^{-1} (average over days 4–6).

4.2.2. Model of EverTREx 3 and 4 at the Fickian Limit

[29] Because EverTREx 3 and 4 reached the Fickian dispersion limit rapidly, the transport model used for these experiments is the advection diffusion equation [*Fischer et al.*, 1979]. As with the SAGED model, this model is extended to include the effects of air-water gas exchange, giving

$$\frac{\partial C}{\partial t} = -\mathbf{U}\nabla C + \mathbf{K}\nabla^2 C - \frac{k_{SF6}}{h} C. \qquad (4)$$

If $\mathbf{U}$ and C are independent of z, and $V = W = 0$, this equation can be simplified to two dimensions. The initial condition is a line release, but given that this line is neither perpendicular to the flow direction nor large compared to the plume scale, the system was modeled with a point release. Solving
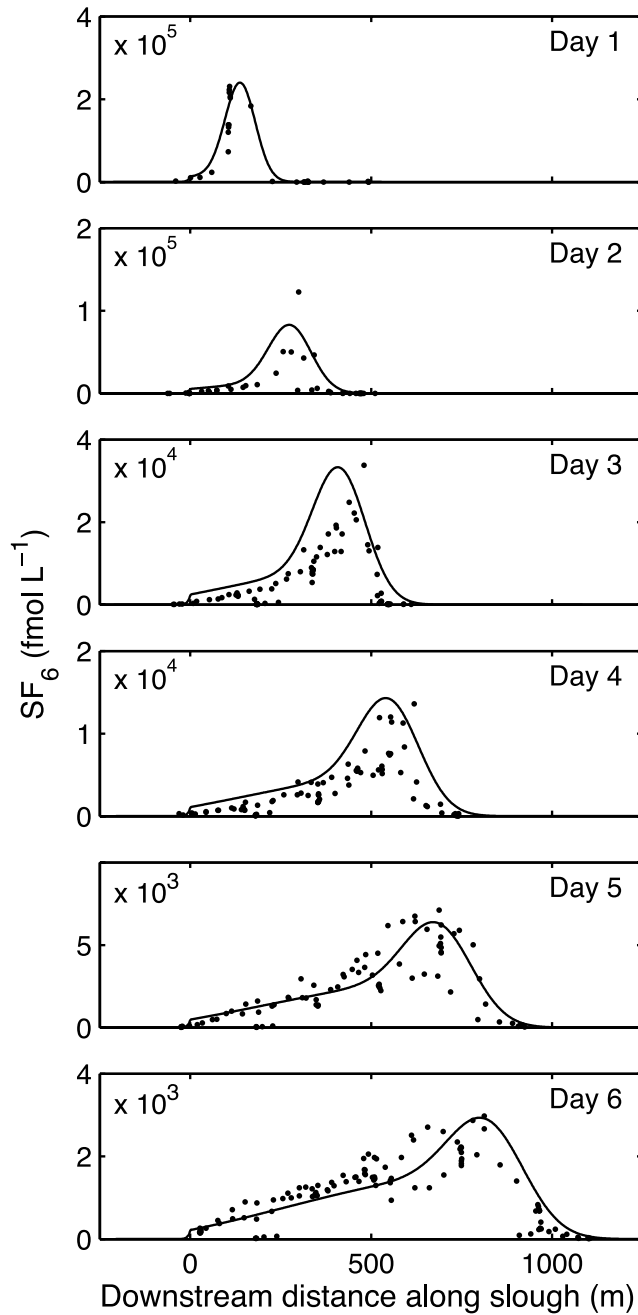
Figure 6. Data from the slough centerline during EverTREx 2 and fitted curves from the SAGED model. Note that the vertical axes are scaled differently in each plot. The uncertainty bounds for each data point (±2% in tracer concentration and ±5 m in location) are not visible at this scale.

equation (4) with Dirichlet boundary conditions and a Dirac delta function initial condition at the origin (center of the tracer release line) having mass M_0 yields the following solution [*Fischer et al.*, 1979]:

$$C(x,y,t) = \frac{M_0}{4\pi t \sqrt{K_x K_y}} \exp\left(-\frac{(x-Ut)^2}{4K_xt} - \frac{y^2}{4K_yt} - \frac{k_{SF6}t}{h}\right). \quad (5)$$

[30] By applying a least squares fit between the model and the measured values of $C(x, y, t)$, the values reported in

Table 6 for EverTREx 3 and 4 were determined. The average daily reduced χ^2 for EverTREx 3 and 4 is 0.4183 and 0.7295, respectively.

5. Discussion

5.1. Advection

[31] Flows during EverTREx were either laminar or transitional, depending on the length scale used to define the Reynolds number. Reynolds number using the plant stem diameter ($\approx$0.5 cm on average) was $Re_d = 7.5$ for EverTREx 2, $Re_d = 3.0$ for EverTREx 3, and $Re_d = 10$ for EverTREx 4. For flow past a cylinder, such values correspond to a completely laminar flow with a trapped recirculating wake. The transition from this steady flow to an unsteady flow occurs at the critical Reynolds number $Re_d \approx 60$ for an isolated cylinder and between 100 and 200 for an array of cylinders [*Cohen and Kundu*, 2004; *Nepf et al.*, 1997b]. Reynolds number based on depth Re_h were 630, 450, and 920 for EverTREx 2, 3, and 4, respectively. For open channel flow, transitional flows are found in the range $500 < Re_h < 12,500$ [*Munson et al.*, 2005].

[32] The absence of turbulent flow does not imply that this flow is easily predictable. On the contrary, the transitional regime exhibits mixing dynamics that are highly variable and sensitive to small changes in flow [*Davidson*, 2004]. This suggests that small changes in flow forcing or vegetation structure can lead to major changes in the dispersion coefficients and drag. Such behavior was observed during EverTREx 1, discussed by *Ho et al.* [2009]. In that experiment, advection and dispersion in neighboring sloughs were quite different despite having the same large-scale forcing. Re_h during EverTREx 1 was between 100 and 960, much of which signifies a transitional flow regime, thus slight differences in stem densities and the relative dominance of plant species between adjacent sloughs may have caused the observed variation. A similar effect is reported by *Huang et al.* [2008], who report a near hundredfold increase in K_x between adjacent landscapes that have identical flow rate (forced by a pump) but different fractions of sawgrass.

[33] The transient storage parameter α should be similarly sensitive to the rate of turbulent mixing and thus highly variable between experiments. This can result in significant changes in skewness due to small changes in the flow and its spatiotemporal distribution, such as that evident in the differences between EverTREx 2 and 3/4.

5.2. Landscape-Scale Drag

[34] The velocities measured during EverTREx can be coupled with EDEN measurements of hydraulic gradient $\frac{\partial \eta}{\partial x}$

Table 5. Advection, Diffusion, Storage, and Gas Exchange Rates Fit to Experimental Data Using the SAGED Model

	EverTREx 2
M_0 (fmol m^{-1})	5.61×10^7
U_F (cm s^{-1})	0.16
U^a (cm s^{-1})	0.15
D_x (cm^2 s^{-1})	100
α (h^{-1})	0.29
β	0.085
k_{SF6} (cm h^{-1})	1.21

aVolume averaged.

Table 6. Advection, Diffusion, and Gas Exchange Rate for the Three Experiments[a]

Field Campaign	U (cm s^{-1})	K_x (cm^2 s^{-1})	K_y (cm^2 s^{-1})	k_{SF6} (cm h^{-1})	C_0 (fmol L^{-1})
EverTREx 2	0.15	[370, 2600]	120	1.21	5.61×10^8
EverTREx 3	0.06	160	30	0.56	1.29×10^8
95% CI	[0.06, 0.07]	[150, 200]	[30, 40]	[0.48, 0.59]	$[1.05, 1.37] \times 10^8$
EverTREx 4	0.20	1800	30	0.27	7.01×10^6
95% CI	[0.17, 0.25]	[770, 3000]	[30, 100]	[0.155, 0.325]	$[5.02, 9.04] \times 10^6$

[a]C_0 is the initial concentration at the tracer release line, computed from M_0 and the release line geometry. EverTREx 2 values are derived from the SAGED model parameters seen in Table 5, other than K_x and K_y, which were determined by *Ho et al.* [2009]. Upper and lower bounds of the 95% confidence intervals (CI) are obtained by the bootstrap method, except for EverTREx 2, where computation costs were prohibitive.

to model the landscape-averaged drag (Table 7) associated with these flow conditions. If this drag is modeled using the Manning equation (assuming infinite channel width), the roughness constant n is found to be larger than the value $0.26 \leq n \leq 0.61$ s m$^{-1/3}$ reported by *Swain et al.* [2004]. This difference may be due to additional sources of drag present at the large scales studied in EverTREx, such as momentum dissipation in lateral shear layers [*White and Nepf*, 2007]. The values of n calculated here are also 4–5 times larger than the values $0.30 \leq n \leq 0.45$ used in the South Florida Water Management Model (South Florida Water Management District, Documentation of the South Florida Water Management Model version 5.5., 2005, West Palm Beach, Florida, available at www.sfwmd.gov).

[35] The Prandtl drag model, as commonly used to evaluate flow through terrestrial canopies [*Finnigan*, 2000, section 6], is

$$\frac{\partial \eta}{\partial x} = \frac{1}{g}\frac{1}{2}C_D a U^2, \quad (6)$$

where C_D is the Re-dependent drag coefficient and a is the frontal vegetation area per unit volume. This model was closed using an empirical expression for C_D based on a single cylinder ($C_D \approx 1 + 10.0 Re_d^{-2/3}$, valid in the interval $1 \leq Re_d \leq 20,000$ [*Saleh*, 2002]). The Prandtl model gives values of $a \in$ [11, 36] for EverTREx 2 and $a \in$ [32, 96] for EverTREx 4 (Table 7). These values are roughly an order of magnitude larger than values of a measured directly in the field, suggesting that further study could be useful, both in methods for parameterizing C_D and for measuring a. Values of a were determined during EverTREx from measurements of biovolume γ (the volume of vegetation per unit water volume) and a simple plant morphology model assuming cylindrical stalks, giving $a = 4\gamma/\pi d$. An average biovolume $\gamma = 3.4$ and 2.4 parts per thousand was measured in EverTREx 2 and 4,

respectively. Using $\gamma \approx 3$ ppt and $d = 0.5 \pm 0.4$ cm gives $a \in$ [0.4, 3.8] m^{-1}. Similar results were found by *Huang et al.* [2008], whose direct measurements of a near the site of EverTREx 2 showed $a \in$ [1.7, 3.8] m^{-1} for a sawgrass ridge and $a \in$ [2.7, 5.8] m^{-1} for a region including a ridge-slough boundary.

[36] The values in Table 7 indicate that the degraded landscape of EverTREx 4 presents more drag to fluid flow than the patterned landscape of EverTREx 2, which will result in smaller flow velocities at a given hydraulic gradient. Increased drag at degraded sites may accelerate the rate at which landscape patterning is further degraded by reducing the variability of flows experienced at a site, thereby changing the sediment flux dynamics.

5.3. Dispersion

[37] The relative importance of advection and dispersion for transport is quantified by the Peclet number, $Pe \equiv U\mathcal{L}/K_x$. The values of Pe computed from all four EverTREx campaigns are between $\mathcal{O}(1)$ and $\mathcal{O}(100)$, as seen in Table 8. *Ho et al.* [2009] also find Peclet numbers in this range, namely, $Pe \in$ [3, 40] for EverTREx 2, which differs from the results reported here because of the use of different velocity estimates (section 4.2.1). These Pe indicate that advection is relatively more important than dispersion, but each process plays a significant role in transport in the Everglades.

[38] The dispersion coefficients measured in EverTREx are larger than other wetland values in the literature [*Lightbody and Nepf*, 2006; *Saiers et al.*, 2003; *Harvey et al.*, 2005; *Huang et al.*, 2008]. The experiment most comparable to EverTREx is that of *Saiers et al.* [2003]. This study occurred in a slough with an identical velocity (0.15 cm s^{-1}), similar depth (60 cm) and similar vegetation (*Eleocharis*, *Utricularia*, and periphyton in "mat" and "sweater" form) to EverTREx 2. Despite these similarities, measured dispersion coefficients varied by several orders of magnitude, with a value of $K_x = 0.44$ cm^2 s^{-1} reported by *Saiers et al.* [2003], and $K_x = $ [370, 2600] cm^2 s^{-1} in

Table 7. Manning and Prandtl Drag Models Evaluated Using Results From EverTREx and USGS EDEN Data[a]

Value	EverTREx 2	EverTREx 4
Inputs		
$\frac{\partial \eta}{\partial x}$	1.21×10^{-5}	5.05×10^{-5}
h (cm)	42	46
U (cm s^{-1})	0.15	0.20
Outputs		
n (s m$^{-1/3}$)	1.30	2.12
a (m^{-1})	28 [11, 36]	74 [32, 96]

[a]Data are not available for EverTREx 3. The range of values for a include the effects of varying the assumed average plant stem diameter d.

Table 8. Peclet Numbers[a]

Field Campaign	Pe[b]
EverTREx 2	[6, 41]
EverTREx 3	40
EverTREx 4	11

[a]Results for EverTREx 2 are computed from the time-varying dispersion coefficients K_x found in work by *Ho et al.* [2009] and the velocity U found in section 4.2.1.

[b]$\mathcal{L} = 1000$ m, a length scale corresponding to the largest features observed during EverTREx.

EverTREx 2 [*Ho et al.*, 2009]. This difference could be partially explained by the highly nonlinear nature of transitional flow (section 5.1). However, the difference in dispersion rates is likely due primarily to the spatial scales of the respective experiments. Landscape variations can cause flow heterogeneities at scales smaller than EverTREx 2, but larger than *Saiers et al.* [2003], that could explain the greater dispersion observed in EverTREx 2.

[39] Similar scale-dependent dispersion has been quantified in turbulent flows [*Richardson and Stommel*, 1948; *Kraichnan and Montgomery*, 1980] and flows through heterogeneous porous media [*Dagan*, 1987; *Gelhar*, 1993]. However, the relationship between K_x and size scale $\mathcal{L}$ has not been well quantified in wetlands. In unbounded turbulent flow, K_x has been observed to grow continuously as $\mathcal{L}^{4/3}$ over a wide range of scales, even beyond the regime where it has been theoretically justified [*Fischer et al.*, 1979]. In saturated flow in porous media, field measurements summarized by *Gelhar et al.* [1992] suggest that the power law growth of K_x with $\mathcal{L}$ changes exponent at a critical value of $\mathcal{L}$. They note, however, that the larger-scale measurements have less reliability. EverTREx provides a method for measuring K_x at very large scales in wetlands, and can serve as an extreme in the continuum of $K_x(\mathcal{L})$. Tracer experiments at scales in between those of EverTREx and other existing measurements are needed to provide a complete picture of $K_x(\mathcal{L})$.

[40] Ideally, both wetland dispersion and its scale dependence can be derived from field-measurable landscape features. Groundwater studies have done this by making use of the variogram to describe spatial variations in permeability [*Gelhar*, 1993]. The analogy in wetlands would be a measure of the spatial autocorrelation of local drag, and the Everglades is an ideal system in which to perform such an analysis. This is because the binary nature of the ridge and slough landscape makes it possible to quantify the spatial distribution of drag using aerial images and a pair of drag values typical of ridges and sloughs. Combining this distribution with an estimate of diffusion rates allows a prediction of K_x following the theory of Taylor [*Fischer et al.*, 1979]. EverTREx data can support this analysis by providing direct measurements of K_x as a reliable point of comparison. Alternately, the EverTREx data can be used to calibrate transport models that operate in inverse mode to derive $U(x, y)$ from landscape geometry. Such a model would provide a velocity field that is consistent with the K_x measured in EverTREx. Such results could be used with Taylor's dispersion model to predict diffusion rates at the EverTREx sites and values of K_x at other locations in the Everglades.

[41] The ratio of longitudinal to lateral dispersion (K_x/K_y) measured during EverTREx was also greater than that reported by *Saiers et al.* [2003]. Their experiments displayed a ratio of 1, while EverTREx 2 displayed a ratio of 3 on days 1–3 and 21.5 on days 4–6 (on average) using values found by *Ho et al.* [2009]. Using the values found in section 4.2.2, EverTREx 3 displayed a ratio of 3 and EverTREx 4 displayed a ratio of 20. This difference between EverTREx and the work of *Saiers et al.* [2003] shows that at larger scales, the variance in u is greater than that in v. This suggests that the additional dispersive mechanism present at large scales increases the along-stream velocity variance more than the cross-stream velocity variance.

5.4. Air-Water Gas Exchange Rate

[42] The gas transfer velocity k_{SF6} is in good agreement with expected values. That is, it is lower than most energetic systems, and on the order of what one sees for gently stirred flows [*Garbe et al.*, 2007]. Most measurements and models focus on the case where gas transfer is dominated by the bed boundary layer or wind forcing. These processes are likely not the key drivers of gas transfer in the Everglades, given the slow flow velocity and the observation that surface wind shear is typically quite small. For example, visual surface signatures during EverTREx corresponded to those expected for Beaufort scale values of 0 or 1 [*Wright et al.*, 1999].

[43] The gas transfer velocity shows statistically significant differences between EverTREx 2, 3, and 4. This difference may be due primarily to differences in rain between the experiments, as enhancement of air-water gas exchange by tropical rain can be significant [*Ho et al.*, 1997, 2000]. Alternative hypotheses are motivated by the observation that the gas transfer velocity is less in the degraded landscapes of EverTREx 3 and 4 than in EverTREx 2. Differences in landscape patterning may influence gas exchange by causing differences in thermal convective mixing, as differential heating of ridges and sloughs can set up horizontal thermal gradients that drive an exchange flow that enhances mixing [*Nepf and Oldham*, 1997; *Oldham and Sturman*, 2001]. Another hypothesis is that different landscape patterns may cause differences in the amount of wind-sheltering and boundary layer dynamics. Studies focused directly on gas transfer would be illuminating, and would require ancillary measurements to investigate these dynamics.

6. Conclusions

[44] SF$_6$ tracer releases were used to investigate the dynamics of surface water flow in a ridge and slough landscape. Flow in a relatively intact ridge and slough habitat was closely aligned with the direction of landscape patterning. In contrast, flow directions in degraded landscapes followed the influence of control structures more closely than the local landscape patterning. Flow that is not aligned with the direction of landscape patterning does not support the sediment transport dynamics that are thought to maintain ridge and slough patterning [*Larsen et al.*, 2007]. Thus by altering flow directions, control structures may accelerate the degradation of patterning such as that seen at the sites of EverTREx 3 and 4. This pattern loss, in turn, contributes to the loss of habitat conducive to wading birds and other characteristic Everglade species.

[45] All three EverTREx data sets showed that both advection and dispersion were important for determining transport, indicated by Peclet numbers between $\mathcal{O}(1)$ and $\mathcal{O}(100)$. Advection was such that Reynolds numbers are in the transitional flow regime, indicating that mixing in the Everglades is sensitive to slight changes in forcing or landscape structure. Dispersion was much larger for EverTREx than that reported in other marsh studies, an effect which can be explained by the unprecedented scale of these measurements. This result indicates that in both degraded and nondegraded landscapes, the hydrodynamic dispersion of substances such as phosphorous may occur more rapidly than would be expected on the basis of measurements at

smaller scales. Furthermore, a comparison of degraded and well-preserved landscapes show that the vegetation in the degraded landscape is more homogeneous and exhibits a greater drag, causing a smaller range of flow velocities in that region.

[46] Future work using the methods of EverTREx could be directed to further evaluate and improve models of vegetative drag by exploring a range of flow conditions and seasonal vegetation changes at one site. Tracer releases could also be performed to evaluate impacts of planned restoration projects entailing changes in engineered flow controls. Finally, the data from EverTREx 1–4 could be used to calibrate and validate transport models that explicitly account for the specific landscape features. Work of this type is currently underway using Lattice-Boltzmann simulations [*Sukop and Thorne*, 2007].

References

Bazante, J., G. Jacobi, H. M. Solo-Gabriele, D. Reed, S. Mitchell-Bruker, D. L. Childers, L. Leonard, and M. Ross (2006), Hydrologic measurements and implications for tree island formation within Everglades National Park, *J. Hydrol.*, *329*, 606–619.

Bencala, K. E., and R. A. Walters (1983), Simulation of solute transport in a mountain pool-and-riffle stream: A transient storage model, *Water Resour. Res.*, *19*(3), 718–724.

Bullister, J. L., D. P. Wisegarver, and F. A. Menzia (2002), The solubility of sulfur hexafluoride in water and seawater, *Deep Sea Res., Part I*, *49*, 175–187.

Cohen, I. M., and P. K. Kundu (2004), *Fluid Mechanics*, 3rd ed., Academic, San Diego, Calif.

Dagan, G. (1987), Theory of solute transport by groundwater, *Annu. Rev. Fluid Mech.*, *19*, 183–213.

Davidson, P. A. (2004), *Turbulence: An Introduction for Scientists and Engineers*, Oxford Univ. Press, New York.

Deans, H. A. (1963), A mathematical model for dispersion in the direction of flow in porous media, *Trans. Soc. Pet. Eng. Am. Inst. Min. Metall. Pet. Eng.*, *228*, 49–52.

Dierberg, F. E., J. J. Juston, T. A. DeBusk, K. Pietro, and B. Gu (2005), Relationship between hydraulic efficiency and phosphorus removal in a submerged aquatic vegetation-dominated treatment wetland, *Ecol. Eng.*, *25*(1), 9–23.

Finnigan, J. (2000), Turbulence in plant canopies, *Annu. Rev. Fluid Mech.*, *32*, 519–571.

Fischer, H. B., J. E. List, C. R. Koh, J. Imberger, and N. H. Brooks (1979), *Mixing in Inland and Coastal Waters*, Academic, San Diego, Calif.

Garbe, C. S., R. A. Handler, and B. Jähne (Eds) (2007), *Transport at the Air-Sea Interface: Measurements, Models and Parameterizations*, Springer, Heidelberg, Germany.

Gelhar, L. W. (1993), *Stochastic Subsurface Hydrology*, Prentice-Hall, Englewood Cliffs, N. J.

Gelhar, L. W., C. Welty, and K. R. Rehfeldt (1992), A critical review of data on field-scale dispersion in aquifers, *Water Resour. Res.*, *28*(7), 1955–1974.

Givnish, T. J., J. C. Volin, V. D. Owen, V. C. Volin, J. D. Muss, and P. H. Glaser (2008), Vegetation differentiation in the patterned landscape of the central Everglades: Importance of local and landscape drivers, *Global Ecol. Biogeogr.*, *17*(3), 384–402.

Grunwald, M. (2006), *The Swamp: The Everglades, Florida, and the Politics of Paradise*, Simon and Schuster, New York.

Harvey, J. W., and B. J. Wagner (2000), Quantifying hydrologic interactions between streams and their subsurface hyporheic zones, in *Streams and Ground Waters*, edited by J. B. Jones and P. J. Mulholland, pp. 3–44, Elsevier, New York.

Harvey, J. W., J. E. Saiers, and J. T. Newlin (2005), Solute transport and storage mechanisms in wetlands of the Everglades, south Florida, *Water Resour. Res.*, *41*, W05009, doi:10.1029/2004WR003507.

Harvey, J. W., R. W. Schaffranek, G. B. Noe, L. G. Larsen, D. J. Nowacki, and B. L. O'Connor (2009), Hydroecological factors governing surface water flow on a low-gradient floodplain, *Water Resour. Res.*, *45*, W03421, doi:10.1029/2008WR007129.

Huang, Y. H., J. E. Saiers, J. W. Harvey, G. B. Noe, and S. Mylon (2008), Advection, dispersion, and filtration of fine particles within emergent vegetation of the Florida Everglades, *Water Resour. Res.*, *44*, W04408, doi:10.1029/2007WR006290.

Ho, D. T., L. F. Bliven, R. Wanninkhof, and P. Schlosser (1997), The effect of rain on air-water gas exchange, *Tellus, Ser. B*, *49*(2), 149–158.

Ho, D. T., W. E. Asher, L. F. Bliven, P. Schlosser, and E. L. Gordan (2000), On mechanisms of rain-induced air-water gas exchange, *J. Geophys. Res.*, *105*(C10), 24,045–24,057.

Ho, D. T., P. Schlosser, and T. Caplow (2002), Determination of longitudinal dispersion coefficient and net advection in the tidal Hudson River with a large-scale, high resolution SF_6 tracer release experiment, *Environ. Sci. Technol.*, *36*(15), 3234–3241.

Ho, D. T., V. C. Engel, E. A. Variano, P. J. Schmieder, and M. E. Condon (2009), Tracer studies of sheet flow in the Florida Everglades, *Geophys. Res. Lett.*, *36*, L09401, doi:10.1029/2009GL037355.

Kraichnan, R. H., and D. Montgomery (1980), Two-dimensional turbulence, *Rep. Prog. Phys.*, *43*(5), 547–619.

Larsen, L. G., J. W. Harvey, and J. P. Crimaldi (2007), A delicate balance: Ecohydrological feedbacks governing landscape morphology in a lotic peatland, *Ecol. Monogr.*, *77*(4), 591–614.

Lee, J. K., L. C. Roig, H. L. Jenter, and H. M. Visser (2004), Drag coefficients for modeling flow through emergent vegetation in the Florida Everglades, *Ecol. Eng.*, *22*, 237–248.

Leonard, L. A., and A. L. Croft (2006), The effect of standing biomass on flow velocity and turbulence in *Spartina alterniflora* canopies, *Estuarine Coastal Shelf Sci.*, *69*, 325–336.

Lightbody, A. F., and H. M. Nepf (2006), Prediction of velocity profiles and longitudinal dispersion in emergent salt marsh vegetation, *Limnol. Oceanogr.*, *51*(1), 218–228.

Munson, B. R., D. Young, and T. H. Okiishi (2005), *Fundamentals of Fluid Mechanics*, 5th ed., John Wiley, New York.

National Research Council (2003), *Does Water Flow Influence Everglades Landscape Patterns?*, Natl. Acad., Washington, D. C.

Nepf, H. M., and C. Oldham (1997), Exchange dynamics of a shallow contaminated wetland, *Aquat. Sci.*, *59*(3), 193–213.

Nepf, H. M., C. G. Mugnier, and R. A. Zavistoski (1997a), The effects of vegetation on longitudinal dispersion, *Estuarine Coastal Shelf Sci.*, *44*, 675–684.

Nepf, H. M., J. A. Sullivan, and R. A. Zavistoski (1997b), A model for diffusion within emergent vegetation, *Limnol. Oceanogr.*, *42*(8), 1735–1745.

Noe, G. B., and D. L. Childers (2007), Phosphorus budgets in Everglades wetland ecosystems: The effects of hydrology and nutrient enrichment, *Wetlands Ecol. Manage.*, *15*(3), 189–205.

Oldham, C. E., and J. J. Sturman (2001), The effect of emergent vegetation on convective flushing in shallow wetlands: Scaling and experiments, *Limnol. Oceanogr.*, *46*(6), 1486–1493.

Richardson, L. F., and H. Stommel (1948), Note on eddy diffusion in the sea, *J. Meteorol.*, *5*(5), 238–240.

Sabol, G. V., and C. F. Nordin (1978), Dispersion in rivers as related to storage zones, *J. Hydraul. Div. Am. Soc. Civ. Eng.*, *104*(5), 695–708.

Saiers, J. E., J. W. Harvey, and S. E. Mylon (2003), Surface-water transport of suspended matter through wetland vegetation of the Florida everglades, *Geophys. Res. Lett.*, *30*(19), 1987, doi:10.1029/2003GL018132.

Saleh, J. (2002), *Fluid Flow Handbook*, McGraw-Hill, New York.

Solo-Gabriele, H. (2008), Documenting the importance of water flow to Everglades landscape structure and sediment transport in Everglades National Park, *Agreement H500000B494 J5297050059*, Univ. of Miami, Miami, Fla.

Sukop, M. C., and D. T. Thorne Jr. (2007), *Lattice Boltzmann Modeling: An Introduction for Geoscientists and Engineers*, Springer, New York.

Swain, E., M. Wolfert, J. Bales, and C. Goodwin (2004), Two-dimensional hydrodynamic simulation of surface-water flow and transport to Florida

Bay through the Southern Inland and Coastal Systems (SICS), *U.S. Geol. Surv. Water Resour. Invest. Rep., 03-4287*, 69 pp.

Taylor, G. I. (1954), The dispersion of matter in turbulent flow through a pipe, *Proc. R. Soc. London, Ser. A*, *223*, 446–468.

Wagner, B. J., and J. W. Harvey (1997), Experimental design for estimating parameters of rate-limited mass transfer: Analysis of stream tracer studies, *Water Resour. Res.*, *33*(7), 1731–1741.

White, B. L., and H. M. Nepf (2007), Shear instability and coherent structures in shallow flow adjacent to a porous layer, *J. Fluid Mech.*, *593*, 1–32.

Wright, J., E. Brown, A. Colling, D. Park, and the Open University Course Team (1999), *Waves, Tides, and Shallow-Water Processes*, Butterworth Heinemann, Milton Keynes, U. K.

Young, W. R., and S. Jones (1991), Shear dispersion, *Phys. Fluids A*, *3*(5), 1087–1101.

————————————

V. C. Engel, South Florida Natural Resources Center, Everglades National Park, 950 North Krome Avenue, Homestead, FL 33030, USA.

D. T. Ho, Department of Oceanography, University of Hawai'i at Mānoa, 1000 Pope Road, MSB 517, Honolulu, HI 96822, USA.

M. C. Reid, Department of Civil and Environmental Engineering, Princeton University, Princeton, NJ 08544, USA.

P. J. Schmieder, Lamont-Doherty Earth Observatory, Earth Institute at Columbia University, Palisades, NY 10964, USA.

E. A. Variano, Department of Civil and Environmental Engineering, University of California, 623 Davis Hall, Berkeley, CA 94720-1710, USA. (variano@ce.berkeley.edu)